

Apoferritin Nanoparticle-Based Mass Tags: A Novel Metal Tagging Strategy for Mass Cytometry

Jinhui Liu, Weiliang Liu, Zhian Hu, Zhi Xing, Gongwei Sun,* Meng Wang,* Sichun Zhang,* and Xinrong Zhang



Cite This: <https://doi.org/10.1021/acs.analchem.5c01918>



Read Online

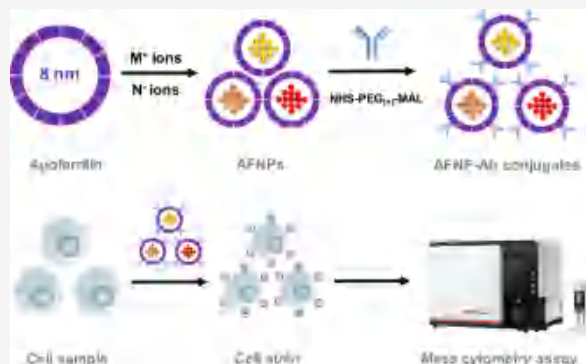
ACCESS |

Metrics & More

Article Recommendations

Supporting Information

ABSTRACT: Mass cytometry (MC), considered the next generation of flow cytometry (FC), uses antibodies tagged with metal isotopes instead of fluorescent molecules for higher-dimensional single cell biomarker assays and can measure more than 50 parameters simultaneously on individual cells. Despite its powerful analytical performance, MC also has limitations in sensitivity and isotope channels using current mass tags. Herein, a new metal tagging strategy was developed to prepare MC mass tags based on apoferritin nanoparticles (AFNPs). For the preparation of AFNPs, rare-earth metals and phosphate ions were sequentially introduced into the cavity of apoferritin by a passive diffusion method to form a metal-phosphate core inside the apoferritin nanocages. The *N*-hydroxysuccinimide polyethylene glycol (MW = 1000, $n = 22$) maleimide (NHS-PEG₂₂-MAL) linker was used to link the AFNPs and antibodies to prepare Ab-NP conjugates. The AFNPs have low nonspecific binding to cells, thus resulting in a low background signal for the MC assay. Under optimized conditions, each apoferritin can load an average of 300–800 rare-earth metal atoms, and AFNP tags have more than twice the sensitivity compared with metal-chelating polymer (MCP) tags. Multiparameter assays for the cellular subset analysis of human peripheral blood mononuclear cells (PBMCs) showed good agreement between FC and MC assays by using our AFNP tags. The study presents a new strategy for preparing MC mass tags that are chelator-independent and have multiple staining capabilities, low nonspecific binding, and high sensitivity. The developed AFNP tags are expected to promote the development of MC technology.



INTRODUCTION

Mass cytometry (MC) is considered the next generation of flow cytometry (FC) technology. It uses metal stable isotope-labeled antibodies instead of traditional fluorescent antibodies for high-dimensional single cell assays, completely avoiding the problems of spectral overlap and autofluorescence in FC.^{1–5} MC can simultaneously detect over 50 biomarkers on millions of individual cells,³ opening a new door for clinical medical research, and has wide applications in immunology and cancer research.^{6–9} While there are 135 theoretical channels for MC, only ~50 channels are actually used.¹⁰ Currently, metal-chelating polymer (MCP) tags, developed by Winnik's group, are the most widely used for MC analysis,^{11,12} and about 46 parameters can be detected simultaneously using the commercial MCP reagents.¹³ The MCP tags bind 20–50 metal ions per polymer, and one antibody can be typically tagged with 2–5 polymers, thus carrying 40–250 metal ions per antibody.^{11,12,14} For MC instruments, only ~1 out of 10⁴ ions generated in the inductively coupled plasma (ICP) can be detected,¹⁰ so hundreds of antigens per cell are required to bind to metal-tagged antibodies to distinguish them from the background signal. In fact, using current MCP tags, MC is

more suitable for detecting biomarkers with abundance >10⁴ per cell.^{10,14} It is a challenge for MC to detect low-abundance biomarkers in single cells. However, current FC instruments can even detect less than 50 molecules of equivalent soluble fluorochrome (MESF) from the parameters provided by FC manufacturers, which is much better than the detection limit of MC. In addition, the preparation procedures of current mass tags are usually complex. Therefore, it is necessary to develop new MC mass tags.

Nanoparticles (NPs) can carry thousands of metal atoms (e.g., 10 nm gold NPs contain about 30 000 gold atoms), making them very promising MC mass tags. At present, some NPs have been tentatively used as MC mass tags, such as gold NPs,¹⁵ silver NPs,¹⁶ quantum dots,¹⁷ polymer dots,¹⁸ lanthanide NPs,^{19,20} tantalum oxide NPs,¹³ metal–organic

Received: March 31, 2025

Revised: June 21, 2025

Accepted: June 24, 2025

frameworks (MOFs),^{21,22} polystyrene NPs,²³ mesoporous silica NPs,²⁴ Lego Brick NPs,²⁵ etc. However, despite numerous attempts, NP tags have not been widely used in MC assays. The main challenge is the nonspecific binding of NPs on cells, which increases the background signal.^{10,19,20,26} Another challenge is the synthesis of NPs. Each type of NP has its own unique synthesis method, and the uniformity of NPs is also difficult to maintain, which makes it difficult to unify and standardize NP tags. In addition, the purification of NP tags is also a challenge, as it is difficult to separate NP-Ab conjugates from mixtures of NP-Ab conjugates, NPs, and antibodies. All of these challenges limit the use of current NPs as MC mass tags, and new NP tags need to be developed.

Apoferitin, deriving from organisms, is composed of 24 protein subunits. These 24 protein subunits first form dimers, and then the dimers self-assemble into a dodecamer nanocage with an external diameter of ~12 nm and an internal cavity of ~8 nm.^{27–29} Due to its unique cage-like cavity structure, apoferitin can be used as a natural nanocontainer to load various materials at the nanoscale, such as inorganic metal oxides and salts, quantum dots, small molecule drugs, platinum-based anticancer drugs, luminescent materials, etc.³⁰ Apoferitin-based nanomaterials have been widely used in drug delivery, sensing, molecular imaging, tumor therapy, etc.^{31,32} Apoferitin-based metal NPs are easily synthesized and chelator-independent, and they have been successfully used to detect biomarkers by electrochemical immunoassay and mass spectrometry immunoassay.^{33–35} Apoferitin-based metal NPs have the advantages of good biocompatibility, uniformity, dispersion, stability, and water-solubility.^{30,31} Based on the above characteristics, we believe that apoferitin-based metal NPs are potential mass tags for MC.

In this work, we develop a new metal isotope tagging strategy where apoferitin NPs (AFNPs) are used as MC mass tags for sensitive and multiparameter single cell biomarker assays. The preparation process of AFNP and antibody (AFNP-Ab) conjugates is shown in Scheme 1. The passive diffusion method was used to introduce rare-earth metal and phosphate ions into the cavity of the apoferitin nanocages in order to form a metal-phosphate core inside the apoferitin

nanocages. *N*-hydroxysuccinimide polyethylene glycol (MW = 1000, *n* = 22) maleimide (NHS-PEG₂₂-MAL) was used as a linker to react the amino groups inherent in AFNPs with *N*-hydroxysuccinimide groups to obtain maleimide-functionalized AFNPs (AFNP-PEG₂₂-MAL). AFNP-Ab conjugates were prepared by reacting the thiol groups of antibodies treated with tris(2-carboxyethyl)phosphine (TCEP) and the maleimide groups of AFNP-PEG₂₂-MAL. The CD45 biomarker on Jurkat T and MCF-7 cells was used to evaluate the nonspecific binding and sensitivity of the AFNP tags. The assays for biomarkers of CD3, CD4, CD8, CD14, CD19, and CD45 in human peripheral blood mononuclear cells (PBMCs) were used to evaluate the multiple staining capability and reliability of the AFNP tags.

EXPERIMENTAL SECTION

Materials and Reagents. Detailed information on apoferitin, antibodies, NHS-PEG₂₂-MAL linker, and the other materials and reagents used in this work is shown in the Supporting Information.

Synthesis of AFNPs. AFNPs were synthesized by the passive diffusion method according to previous reports with some modifications.^{33–36} The details are shown in the Supporting Information.

Preparation of Maleimide-Functionalized AFNPs. First, 10 μ L of NHS-PEG₂₂-MAL solution with a concentration of 50 mM was added to 100 μ L of the above AFNPs solution. The reaction was kept for 2 h at 37 $^{\circ}$ C, and the excess NHS-PEG₂₂-MAL was removed by ultrafiltration centrifugation (12 000 rpm, MWCO = 100 kDa) using PBS to prepare maleimide-functionalized AFNPs. The maleimide-functionalized AFNPs were reconstituted into 200 μ L of PBS for the next experiment.

Preparation of AFNP-Ab Conjugates. The commercial antibodies (anti-CD3, anti-CD4, anti-CD8, anti-CD14, anti-CD19, and anti-CD45) were first washed 2 times using PBS with ultrafiltration centrifugation (12 000 rpm, MWCO = 30 kDa). Subsequently, 100 μ L of TCEP solution (5 mM) was added to each 100 μ L antibody solution (about 100 μ g of antibody) to activate the thiol functional groups of the antibodies. The reaction was kept for 30 min at 37 $^{\circ}$ C, and the excess TCEP was then removed with ultrafiltration centrifugation (12 000 rpm, MWCO = 30 kDa). Then, 50 μ L of maleimide-functionalized AFNPs (0.25 mg/mL) and different volumes of thiol-activated antibody (1 mg/mL) were mixed to prepare AFNP-Ab conjugates; the reaction was kept for 2 h at 37 $^{\circ}$ C. Finally, PBS and bovine serum albumin (BSA) were added to the AFNP-Ab conjugate solution to form a final volume of 300 μ L with 1% BSA (w/v).

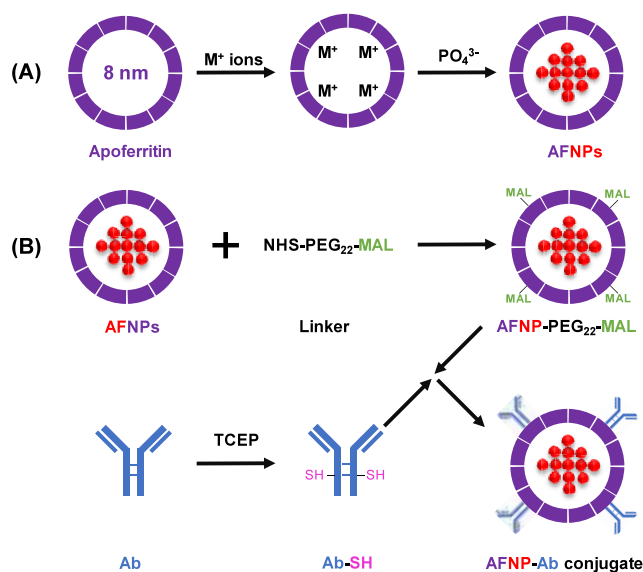
Cell Culture and Stain. Jurkat T cells, MCF-7 cells, and PBMCs were used in this work. The details are shown in the Supporting Information.

MC Measurements. An MC instrument (MSFLO, Hangzhou POWCLIN Medical Technology Co., Ltd., China) was used in this work. The details are shown in the Supporting Information.

RESULTS AND DISCUSSION

Synthesis and Characterization of AFNPs. AFNPs were synthesized by the passive diffusion method,^{33–36} as shown in Scheme 1A. Rare-earth metal ions were first introduced into the cavity of apoferitin, and phosphate ions were subsequently

Scheme 1. Preparation Process of AFNP-Ab Conjugates



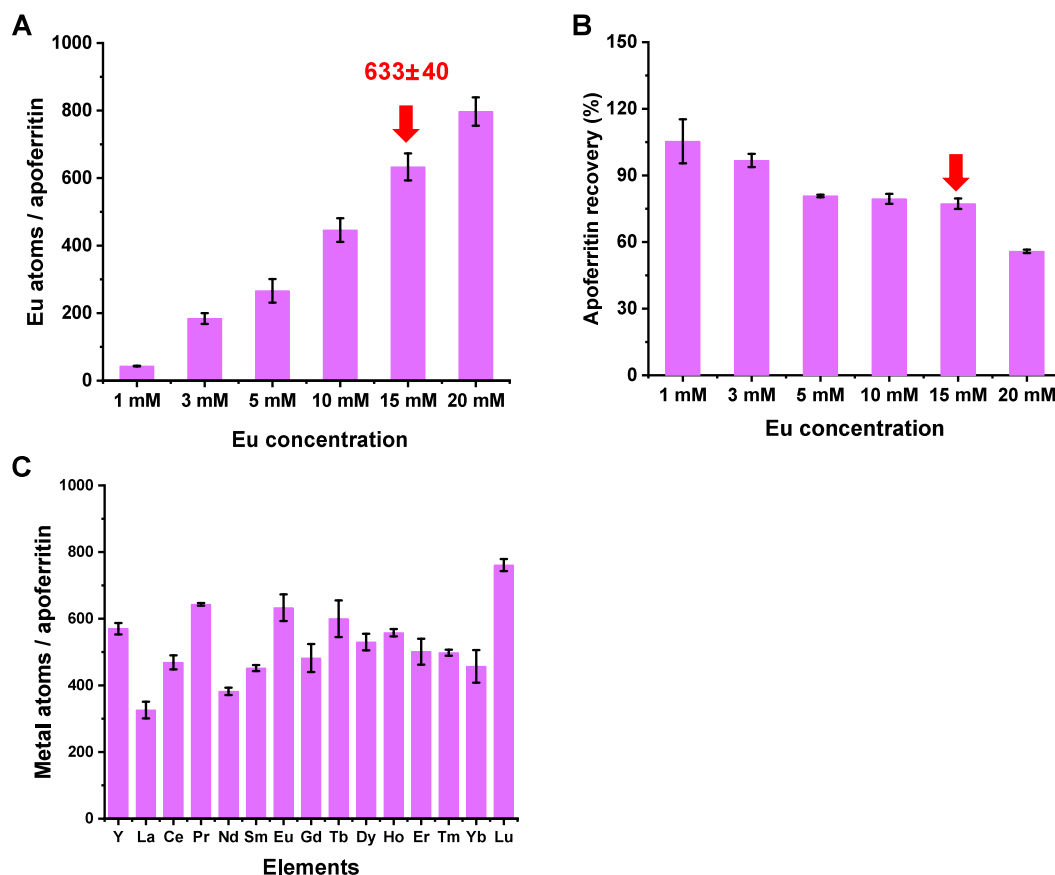


Figure 1. (A) Histogram of the number of Eu atoms loaded in each apoferritin for different Eu concentrations used to synthesize AFNPs ($n = 3$). (B) Histogram of the recovery of apoferritin for different Eu concentrations used to synthesize AFNPs ($n = 3$). (C) Histogram of the number of metal atoms loaded in each apoferritin for different rare-earth metals used to synthesize AFNPs with a metal concentration of 15 mM ($n = 3$).

introduced to form a rare-earth metal-phosphate core in the cavity of apoferritin. Lanthanide phosphates have shown their stability in microgels.³⁷ In order to achieve an optimal loading capacity for rare-earth metals in the apoferritin cavity, we referred to the method of Lin et al.³⁶ Different concentrations (1, 3, 5, 10, 15, and 20 mM) of Eu nitrate were used for the synthesis of AFNPs (Eu core) in the initial steps. The number of rare-earth metals loaded inside apoferritin was calculated by measuring the concentrations of apoferritin and rare-earth metals of the apoferritin solutions.

An ultratrace nucleic acid and protein spectrophotometer was used for the measurement of the apoferritin protein concentration. Figure S1A shows the UV spectra of apoferritin (black) and AFNPs (red) with a concentration of about 0.3 mg/mL, as measured by an ultratrace nucleic acid and protein spectrophotometer at wavelengths ranging from 220 to 350 nm. The results showed that the UV spectra of apoferritin and AFNPs are nearly identical, and they both exhibited a maximum UV absorption peak at 280 nm. Figure S1B shows the calibration curve of apoferritin solution at concentrations of 0, 0.1, 0.2, 0.5, 1.0, and 2.0 $\mu\text{g/mL}$, which shows good linearity ($R^2 > 0.999$). MC quantitative analysis mode was used for the measurement of the rare-earth metal content of the AFNP solutions. The average number of rare-earth metal atoms contained in AFNPs can be calculated by dividing the number of metal atoms by the number of ferritin nanoparticles in the AFNP solution. Figure 1A shows the histogram of the number of Eu loaded in apoferritin when different Eu concentrations were used to synthesize Eu core AFNPs ($n =$

3). We found that the Eu atoms loaded in apoferritin increased with higher concentrations of Eu ions used in the synthesis. However, high metal concentrations can cause the aggregation of apoferritin, resulting in the loss of apoferritin.³⁶ Figure 1B shows the recovery of apoferritin when different Eu concentrations were used to synthesize Eu core AFNPs ($n = 3$). We found that the recovery of apoferritin was approximately 80% for the use of 15 mM Eu and only 55% for the use of 20 mM Eu. To achieve a compromise between the number of Eu loaded and the recovery of apoferritin, we chose a 15 mM rare-earth metal concentration to synthesize all of the types of AFNPs in this work. When using 15 mM Eu to synthesize AFNPs, an average of 633 ± 40 Eu atoms were loaded into each apoferritin, which is consistent with a previous report.³⁶ Under the metal concentration of 15 mM, we synthesized 15 kinds of AFNPs with common rare-earth metal elements (Y, La, Ce, Pr, Nd, Sm, Eu, Gd, Tb, Dy, Ho, Er, Tm, Yb, and Lu), and Figure 1C shows the histogram of the number of different rare-earth metal atoms loaded in each AFNP ($n = 3$). The results showed that each apoferritin was loaded with an average of 300–800 metal atoms for different rare-earth metals, which is 2–5 times the number of metal atoms loaded per antibody conjugate for MCP tags (about 150).¹⁰

Figure S2 shows typical transmission electron microscopy (TEM) images of the AFNPs widely used in this work. No aggregates of these AFNPs were observed in the TEM images, suggesting good monodispersity of AFNPs in aqueous environments. All kinds of AFNPs with different metal cores

(Tm, Y, Pr, Eu, Tb, Ho, Lu) have a similar size, and the Tm core AFNPs have a uniform diameter of 7.4 ± 2.5 nm, which is consistent with the theoretical diameter.³¹

Preparation of AFNP-Ab Conjugates. The preparation process of AFNP-Ab conjugates is shown in Scheme 1B. For the preparation of MC mass tags, the link of materials loading metal isotopes and antibodies is a critical part. Since AFNPs cannot directly react or adsorb with antibodies, the linkers between AFNPs and antibodies are indispensable. As far as we know, *N*-hydroxysuccinimide groups can be used to label the amino groups of proteins to form a stable amide bond structure. Considering that apoferritin itself is a type of protein, its surface is rich in amino groups, so the *N*-hydroxysuccinimide group can be used as one end of the linker. The maleimide groups can react with thiol groups to form covalent bonds, enabling the connection of biomolecules using thiol groups and maleimide groups, which have been successfully used to link MCPs and antibodies for MCP tags.¹¹ Therefore, we chose a maleimide group as the other end of the link. In addition, to avoid steric hindrance effects, we introduced water-soluble poly(ethylene glycol) (PEG) between the *N*-hydroxysuccinimide groups and the maleimide groups. Based on the above considerations, we chose NHS-PEG₂₂-MAL as the linker to connect AFNPs and antibodies, and Figure S3 shows the structural formula of the NHS-PEG₂₂-MAL linker. We first coincubated NHS-PEG₂₂-MAL and AFNPs, and the excess NHS-PEG₂₂-MAL was removed by ultrafiltration centrifugation (12 000 rpm, MWCO = 100 kDa), thus obtaining AFNP-PEG₂₂-MAL. Subsequently, we used TCEP to activate the thiol groups on the antibodies. Finally, we coincubated the thiol-activated antibodies with AFNP-PEG₂₂-MAL to obtain AFNP-Ab conjugates. Figure S4 shows the dynamic light scattering (DLS) measurement results of AFNPs, AFNP-PEG₂₂-MAL, and AFNP-Ab, which indicated that the hydrodynamic size of AFNPs changed from 17 to 24 nm after NHS-PEG₂₂-MAL modification and to 43 nm after antibody conjugation. These results indicated that we had prepared AFNP-Ab conjugates. Figure S5 shows the ¹H NMR spectra of AFNPs, NHS-PEG₂₂-MAL, and AFNP-PEG₂₂-MAL. By comparing the characteristic peak of the chemical shift at 7.82 ppm, we calculated that each AFNP could link about 51 NHS-PEG₂₂-MAL linkers on average.

For the preparation of MC mass tags, it is necessary to remove the excess unconjugated antibodies or metal loading materials because free antibodies will compete with conjugates for the binding sites on cells and free metal loading materials will increase the background signal. In the preparation process of MCP tags, the MCPs were in excess, and the excess MCPs were removed by ultrafiltration centrifugation.¹¹ In the preparation process of NP tags, antibodies were usually in excess, and excess antibodies can be centrifuged to remove the supernatant, such as MOFs and NaLnF₄ NPs.^{19,21} However, for NPs with small sizes or relatively low density, excess antibodies are difficult to remove by routine centrifugation, and the purification of these NP-Ab conjugates requires other strategies. For example, tantalum oxide NP tags (~5.7 nm) were purified by fast protein size exclusion liquid chromatography (FPLC).¹³ However, the FPLC process is relatively complex and will result in the loss of NP-Ab conjugates.

Herein, we designed a titration experiment to determine the optimal binding ratio of antibodies and AFNPs, thus avoiding the experimental process of purification. The CD45 biomarker

on human Jurkat T cells was used as a research model. 0, 3.75, 18.75, 30, 37.5, 75, and 187.5 μ L of antibody solution (anti-CD45, 1 mg/mL) and 50 μ L AFNPs (Tm core, 0.25 mg/mL) were mixed to form the molar ratios of antibody to AFNPs of 0:1, 1:1, 5:1, 8:1, 10:1, 20:1, and 50:1 for the preparation of AFNP-Ab conjugates, respectively. BSA and PBS were added to make the final volume 300 μ L, with 1% BSA. Subsequently, these AFNP-Ab conjugates were used to stain human Jurkat T cells (2 μ L for 1 million cells). Figure 2A shows the MC

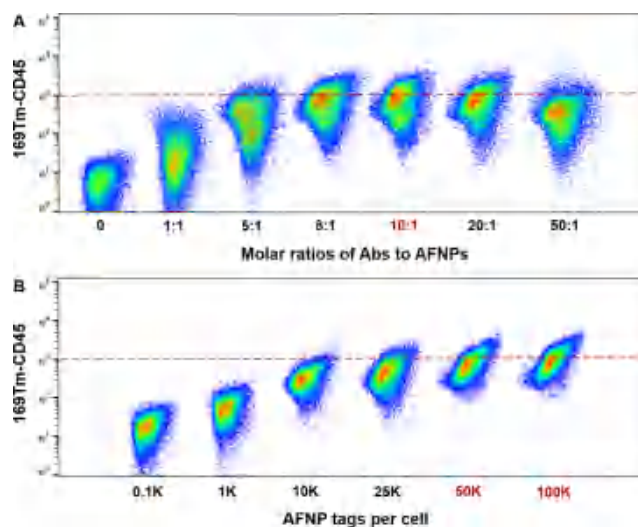


Figure 2. Measurement results for the human Jurkat T cells stained with (A) AFNP-Ab conjugates at different molar ratios of antibodies to AFNPs and (B) AFNP tags at different concentrations.

measurement results for the human Jurkat T cells stained with different AFNP-Ab conjugates (¹⁶⁹Tm-CD45), and Table S2 show the mean ¹⁶⁹Tm signal intensity for different staining conditions. The ¹⁶⁹Tm signal intensity of CD45 on the human Jurkat T cells increases with the ratio of antibodies to AFNPs increasing from 0:1 to 10:1, reaching a maximum value (mean: 1039) at 10:1. When it exceeds 10:1 to 20:1, the ¹⁶⁹Tm signal intensity of CD45 slightly decreases (mean: 876), and at 50:1, the signal intensity decreases more significantly (mean: 454). The results are consistent with the theory that excess antibodies compete with AFNP-Ab conjugates for binding sites on cells, thereby reducing the signal sensitivity of CD45 on human Jurkat cells. Therefore, in subsequent experiments, we chose a binding ratio of 10:1 between the antibodies and AFNPs to prepare AFNP-Ab conjugates.

Optimization of Staining Concentration of AFNP Tags.

For the cell staining, an appropriate concentration of the MC tag is necessary. This is because an insufficient concentration of MC tags will result in a low signal, and an excessive concentration may increase the cleaning steps and the background signal. For concentration titration, human Jurkat T cells were stained with AFNP tags (¹⁶⁹Tm-CD45) in dosages of 100, 1000, 10 000, 25 000, 50 000, and 100 000 AFNPs/cell. Figure 2B shows the MC measurement results for the human Jurkat T cells stained with different concentrations of the AFNP tag (¹⁶⁹Tm-CD45). The results indicated that the signal intensity of CD45 on the human Jurkat T cells increases with the concentration of AFNP tags. However, in actual measurement, when the Jurkat T cells were stained with over 100 000 AFNPs/cell, the MC instrument may experience signal overload and needs to be washed more times to remove

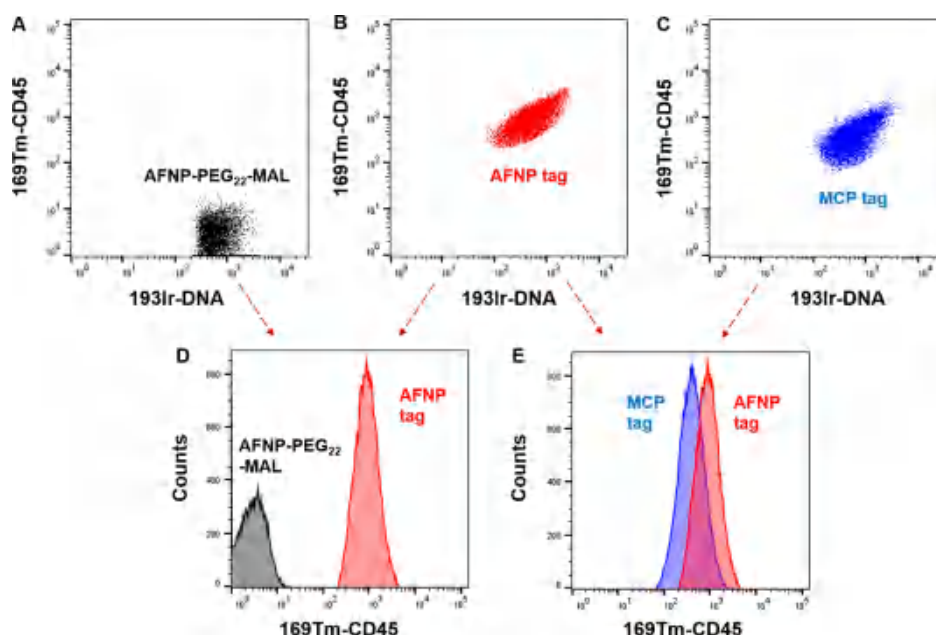


Figure 3. MC measurement results for the human Jurkat T cells stained with (A) AFNP-PEG₂₂-MAL (¹⁶⁹Tm), (B) AFNP tags (¹⁶⁹Tm-CD45), and (C) MCP tags (¹⁶⁹Tm-CD45); (D) the comparison result of ¹⁶⁹Tm signal intensity of human Jurkat T cells stained with AFNP-PEG₂₂-MAL (¹⁶⁹Tm) and AFNP tag (¹⁶⁹Tm-CD45); and (E) the comparison result of ¹⁶⁹Tm signal intensity of the human Jurkat T cells stained with AFNP tags (¹⁶⁹Tm-CD45) and MCP tags (¹⁶⁹Tm-CD45).

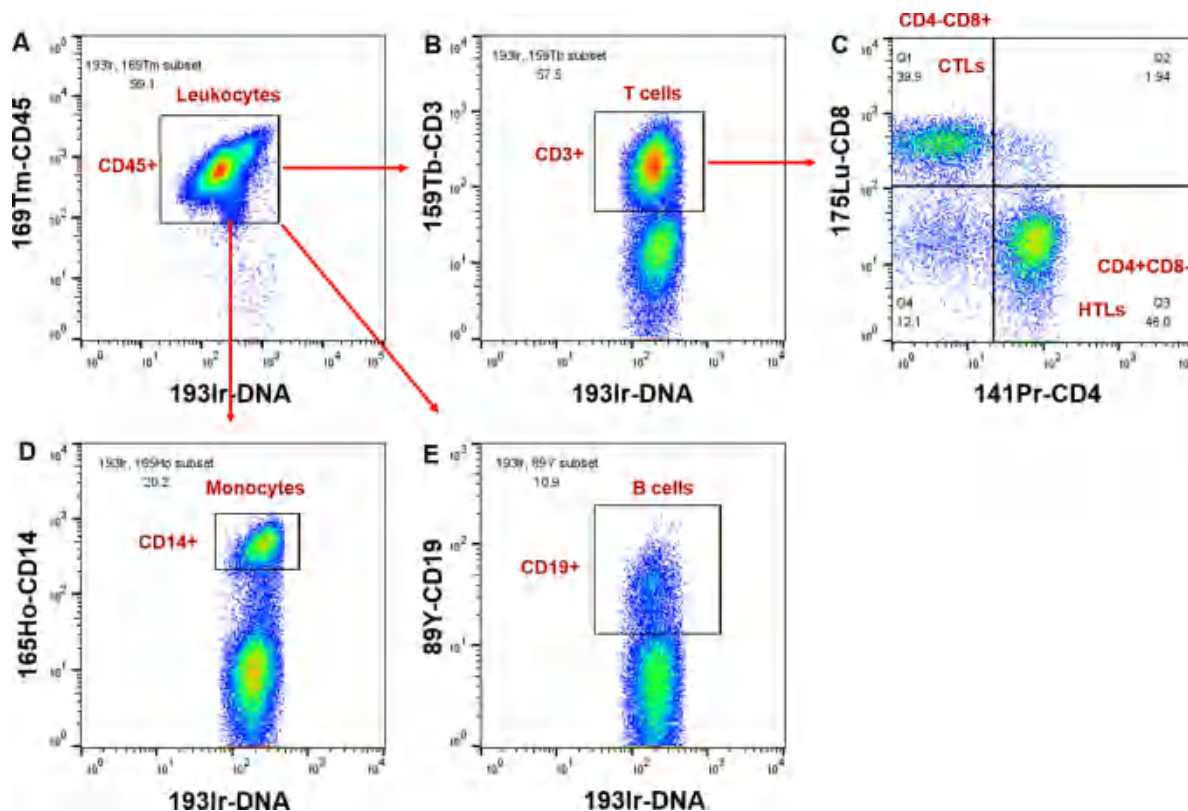


Figure 4. Results of the multiparameter assays of PBMCs stained with AFNP tags obtained from the MC measurement. (A) Logic Gate of CD45+ for leukocytes; (B) Logic Gate of CD45+CD3+ for T cells; (C) Logic Gates of CD45+CD3+CD4+CD8− for helper T lymphocytes (HTLs) and CD45+CD3+CD4−CD8+ for cytotoxic T lymphocytes (CTLs); (D) Logic Gate of CD45+CD14+ for monocytes; (E) Logic Gate of CD45+CD19+ for B cells.

free AFNP tags. Furthermore, when Jurkat T cells were stained with 50 000 AFNPs/cell, the ¹⁶⁹Tm signal intensity can reach an approximate level of that of cells stained with 100 000

AFNPs/cell (see Figure S6). It is worth noting that, when staining with 100 000 AFNPs/cell, an additional one or two washes are necessary compared to using 50 000 AFNPs/cell.

Therefore, we suggest a cell staining concentration ranging from 50 000 to 100 000 AFNP tags/cell.

Nonspecific Binding and Sensitivity of AFNP Tags.

The background signal caused by the nonspecific binding of NPs to cells is a crucial issue limiting the use of NP tags.^{10,19}

To evaluate the nonspecific binding and sensitivity of our AFNP tags, the CD45 biomarker on human Jurkat T (CD45+) and MCF-7 (CD45-) cells was used as a research model, as CD45 is a type of highly expressed protein in human Jurkat T cells.³⁸ We used AFNPs without bonding antibodies (AFNP-PEG₂₂-MAL, Tm core), AFNP tags (¹⁶⁹Tm-CD45), and MCP tags (¹⁶⁹Tm-CD45) to stain the CD45 biomarker on human Jurkat T cells, respectively. Figure 3 shows the MC measurement results for the human Jurkat T cells stained with different tags. Figure 3 A–C presents the ¹⁶⁹Tm signal in Jurkat T cells stained with AFNP-PEG₂₂-MAL (¹⁶⁹Tm), AFNP tag (¹⁶⁹Tm-CD45), and MCP tag (¹⁶⁹Tm-CD45), respectively. Figure 3A indicates that there is very low ¹⁶⁹Tm signal intensity in Jurkat T cells stained with AFNP-PEG₂₂-MAL (¹⁶⁹Tm), and the mean signal intensity of ¹⁶⁹Tm is only 2.18. Figure 3B shows that Jurkat T cells stained with our AFNP tag (¹⁶⁹Tm-CD45) have an obvious signal intensity of ¹⁶⁹Tm, up to a mean of 980, 450-fold that of the Jurkat T cells stained with AFNP-PEG₂₂-MAL (¹⁶⁹Tm). The results indicated that AFNPs have low nonspecific binding to cells. The mean signal intensity of ¹⁶⁹Tm of the Jurkat T cells stained with the MCP tag is 456, about half of the signal intensity of the Jurkat T cells stained with AFNP tags. The obvious comparison results are shown in Figure 3D,E. We also used AFNP tags (¹⁶⁹Tm-CD45) and MCP tags (¹⁶⁹Tm-CD45) to stain the CD45 biomarker on MCF-7 cells. Figure S7 shows the comparison results for the two tags. The mean ¹⁶⁹Tm signal intensity for the MCF-7 cells stained with AFNP tags is 20.8, about 3 times that of the cells stained with MCP tags (7.5). This difference may be due to the AFNP tags carrying more metal atoms. Theoretically, AFNP tags will cause 2–5 times the signal intensity of MCP tags for each antibody conjugate adsorbed in one cell. Our results are consistent with the expectation. The results indicate that the AFNP tags we prepared have a low nonspecific binding to cells and, more importantly, have higher sensitivity than MCP tags.

Multiparameter Assays of PBMCs Stained with AFNP Tags. A prominent feature of MC is single cell multiparameter assays; therefore, we measure 6 biomarkers in PBMCs to evaluate the multiple staining ability of our AFNP tags. MC and FC have been used to analyze PBMCs to provide comparable results for the cellular multiparameter biomarker assays, which provide approximate phenotype results of PBMCs.^{18,39} Therefore, we compare the two measurement results to verify the reliability of our AFNP tags. Herein, we chose biomarkers of CD3, CD4, CD8, CD14, CD19, and CD45 to investigate the cell phenotypes of leukocytes, T cells, B cells, monocytes, helper T lymphocytes (HTLs), and cytotoxic T lymphocytes (CTLs) in PBMCs. The correspondence of antibodies and metal isotopes for AFNP tags is shown in Table S3. We first prepared a 6-complex AFNP-Ab staining cocktail containing anti-CD3, anti-CD4, anti-CD8, anti-CD14, anti-CD19, and anti-CD45 tags, which was then used to stain PBMCs. Figure 4 shows the results of the multiparameter assays of PBMCs stained with AFNP tags from the MC measurement. All cellular subsets of interest (leukocytes, T cells, B cells, monocytes, HTLs, and CTLs) in PBMCs can be clearly distinguished for cellular staining using our AFNP tags.

Table 1 shows the comparison results of cellular subsets of PBMCs obtained from the FC assays (Figure S5) and the MC

Table 1. Comparison of Results of Cellular Subsets of PBMCs Obtained from Flow Cytometry Assays and MC Assays Staining with AFNP Tags

Logic Gate	Biomarkers	Cell Subsets	FCA ^a (%)	MCA ^b (%)
PBMCs	CD45+	Leukocytes	98.9	99.1
In CD45+	CD3+	T cells	55.4	57.5
	CD14+	Monocytes	17.5	20.2
	CD19+	B cells	13.9	10.9
In CD3+	CD4+CD8-	HTLs	47.9	46.0
	CD4-CD8+	CTLs	41.0	39.9

^aFlow cytometry assay results of PBMCs, provided by Milecell Biological Science & Technology Co., Ltd. (Figure S5). ^bMass cytometry assay results of PBMCs stained with AFNP tags.

assays stained with AFNP tags. The results of the two methods for cellular subsets of PBMCs showed good consistency. The results indicated that our synthesized AFNP tags have multiple staining capability for cells to perform multiparameter assays of single cell biomarkers with good reliability.

CONCLUSIONS

In conclusion, we have developed a new mass tag based on AFNPs for single cell biomarker MC assays. The AFNPs can be easily synthesized by a passive diffusion method and easily coupled to thiol-activated antibodies by an NHS-PEG₂₂-MAL linker to prepare AFNP tags, thus simplifying the preparation process of MC mass tags. Each apoferritin can load an average of 300–800 rare-earth metal atoms, 2–5 times of that for MCP tags (~150 metal atoms). Under an optimized binding ratio of antibodies to AFNPs, as well as an optimized staining concentration, AFNP tags have more than twice the sensitivity compared to MCP tags. In addition, AFNPs have a low level of nonspecific binding with cells, resulting in a low background signal. The multiparameter assays for the cellular subsets of PBMCs stained with our AFNP tags show good agreement with the flow cytometry assays, confirming the reliability and multiple staining capability of our AFNP tags. These results demonstrate that our AFNP tags can be used in single cell MC assays, especially in multiparameter assays, which is expected to promote the development of MC technology. In the future, we strongly believe that our AFNP tags will be routinely used in MC assays and will be expanded into the use of tagging non-rare-earth metal elements and imaging mass cytometry.

ASSOCIATED CONTENT

Supporting Information

The Supporting Information is available free of charge at <https://pubs.acs.org/doi/10.1021/acs.analchem.5c01918>.

Materials and reagents; synthesis of AFNPs; cell culture and stain; MC measurements; parameters of the mass cytometry; UV spectra of apoferritin and AFNPs; TEM images of AFNPs; structural formula of the NHS-PEG₂₂-MAL linker; DLS of AFNPs; 1H NMR measurement of AFNPs; average ¹⁶⁹Tm signal intensity for different staining conditions; ¹⁶⁹Tm signal in Jurkat T cells stained with different AFNP tag concentrations; MCF-7 and T cell staining with AFNP tags and MCP tags; the correspondence of antibodies and metal isotopes for

AFNP tags; and the results of the multiparameter assays of PBMCs using flow cytometry (PDF)

AUTHOR INFORMATION

Corresponding Authors

Gongwei Sun – Division of Chemical Metrology and Analytical Science, National Institute of Metrology, Beijing 100029, China; Email: sungw@nim.ac.cn

Meng Wang – CAS Key Laboratory for Biomedical Effects of Nanomaterials and Nanosafety, Institute of High Energy Physics, Chinese Academy of Sciences, Beijing 100049, China; orcid.org/0000-0002-4970-8590; Email: wangmeng@ihep.ac.cn

Sichun Zhang – Department of Chemistry, Tsinghua University, Beijing 100084, China; State Key Laboratory of Analytical Chemistry for Life Science, School of Chemistry and Chemical Engineering, Nanjing University, Nanjing 210093, China; orcid.org/0000-0001-8927-2376; Email: sczhang@mail.tsinghua.edu.cn

Authors

Jinhui Liu – Department of Chemistry, Tsinghua University, Beijing 100084, China; orcid.org/0000-0003-2052-877X

Weiliang Liu – Department of Chemistry, Tsinghua University, Beijing 100084, China

Zhian Hu – University of Science and Technology Beijing, Beijing 100083, China; orcid.org/0000-0002-4475-1477

Zhi Xing – Department of Chemistry, Tsinghua University, Beijing 100084, China; orcid.org/0000-0002-0313-3509

Xinrong Zhang – Department of Chemistry, Tsinghua University, Beijing 100084, China

Complete contact information is available at:

<https://pubs.acs.org/10.1021/acs.analchem.5c01918>

Notes

The authors declare no competing financial interest.

ACKNOWLEDGMENTS

We acknowledge the support by the National Science and Technology Major Project of the Ministry of Science and Technology of China (2022YFF0710200), the National Natural Science Foundation of China (Grants 22404093), Beijing Natural Science Foundation (Grants Z230008 and 2252014), the Postdoctoral Foundation of Tsinghua-Peking Center for Life Sciences, the NIM Research Project (AKYZZ2447), the China Postdoctoral Science Foundation (Grants GZC20231252), and the Open Research Fund of State Key Laboratory of Analytical Chemistry for Life Science, School of Chemistry and Chemical Engineering, Nanjing University. Special thanks are given for the instrumental analysis provided by the Tsinghua University Analysis Center.

REFERENCES

- (1) Bandura, D. R.; Baranov, V. I.; Ornatsky, O. I.; Antonov, A.; Kinach, R.; Lou, X.; Pavlov, S.; Vorobiev, S.; Dick, J. E.; Tanner, S. D. *Anal. Chem.* **2009**, *81* (16), 6813–6822.
- (2) Spitzer, M. H.; Nolan, G. P. *Cell* **2016**, *165* (4), 780–791.
- (3) Han, G.; Spitzer, M. H.; Bendall, S. C.; Fantl, W. J.; Nolan, G. P. *Nat. Protoc.* **2018**, *13* (10), 2121–2148.
- (4) Newell, E. W.; Cheng, Y. *Nature Immunology* **2016**, *17* (8), 890–895.
- (5) Chang, P. P.; Zheng, L. N.; Wang, B.; Chen, M. L.; Wang, M.; Wang, J. H.; Feng, W. Y. *Atomic Spectroscopy* **2022**, *43* (3), 255–265.
- (6) Bendall, S. C.; Simonds, E. F.; Qiu, P.; Amir, E. A. D.; Krutzik, P. O.; Finck, R.; Bruggner, R. V.; Melamed, R.; Trejo, A.; Ornatsky, O. I.; et al. *Science* **2011**, *332* (6030), 687–696.
- (7) Giesen, C.; Wang, H. A. O.; Schapiro, D.; Zivanovic, N.; Jacobs, A.; Hattendorf, B.; Schüffler, P. J.; Grolimund, D.; Buhmann, J. M.; Brandt, S.; et al. *Nat. Methods* **2014**, *11* (4), 417–422.
- (8) Winter, D. R.; Ledergor, G.; Amit, I. *Nat. Biotechnol.* **2015**, *33* (9), 931–932.
- (9) Simoni, Y.; Chng, M. H. Y.; Li, S. M.; Fehlings, M.; Newell, E. W. *Current Opinion in Immunology* **2018**, *51*, 187–196.
- (10) Arnett, L. P.; Rana, R.; Chung, W. W.-Y.; Li, X.; Abtahi, M.; Majonis, D.; Bassan, J.; Nitz, M.; Winnik, M. A. *Chem. Rev.* **2023**, *123* (3), 1166–1205.
- (11) Lou, X.; Zhang, G.; Herrera, I.; Kinach, R.; Ornatsky, O.; Baranov, V.; Nitz, M.; Winnik, M. A. *Angew. Chem., Int. Ed.* **2007**, *46* (32), 6111–6114.
- (12) Majonis, D.; Herrera, I.; Ornatsky, O.; Schulze, M.; Lou, X.; Soleimani, M.; Nitz, M.; Winnik, M. A. *Anal. Chem.* **2010**, *82* (21), 8961–8969.
- (13) Zhang, Y.; Zabinyakov, N.; Majonis, D.; Bouzekri, A.; Ornatsky, O.; Baranov, V.; Winnik, M. A. *Anal. Chem.* **2020**, *92* (8), 5741–5749.
- (14) Ily, N.; Majonis, D.; Herrera, I.; Ornatsky, O.; Winnik, M. A. *Biomacromolecules* **2012**, *13* (8), 2359–2369.
- (15) Malile, B.; Brkic, J.; Bouzekri, A.; Wilson, D. J.; Ornatsky, O.; Peng, C.; Chen, J. I. L. *ACS Applied Bio Materials* **2019**, *2* (10), 4316–4323.
- (16) Schulz, A. R.; Stanislawiak, S.; Baumgart, S.; Grützkau, A.; Mei, H. E. *Cytometry Part A* **2017**, *91* (1), 25–33.
- (17) Newell, E. W.; Sigal, N.; Bendall, S. C.; Nolan, G. P.; Davis, M. M. *Immunity* **2012**, *36* (1), 142–152.
- (18) Wu, X.; DeGottardi, Q.; Wu, I.-C.; Yu, J.; Wu, L.; Ye, F.; Kuo, C.-T.; Kwok, W. W.; Chiu, D. T. *Angew. Chem., Int. Ed.* **2017**, *56* (47), 14908–14912.
- (19) Pichaandi, J.; Zhao, G.; Bouzekri, A.; Lu, E.; Ornatsky, O.; Baranov, V.; Nitz, M.; Winnik, M. A. *Chemical Science* **2019**, *10* (10), 2965–2974.
- (20) Pichaandi, J.; Tong, L.; Bouzekri, A.; Yu, Q.; Ornatsky, O.; Baranov, V.; Winnik, M. A. *Chem. Mater.* **2017**, *29* (11), 4980–4990.
- (21) Dang, J.; Li, H.; Zhang, L.; Li, S.; Zhang, T.; Huang, S.; Li, Y.; Huang, C.; Ke, Y.; Shen, G.; et al. *Adv. Mater.* **2021**, *33* (35), No. 2008297.
- (22) Chen, Y.; Wang, G.; Wang, P.; Liu, J.; Shi, H.; Zhao, J.; Zeng, X.; Luo, Y. *Angew. Chem., Int. Ed.* **2022**, *61* (38), No. e202208640.
- (23) Liu, Z.; Yang, Y.; Zhao, X.; Wang, T.; He, L.; Nan, X.; Vidović, D.; Bai, P. *J. Colloid Interface Sci.* **2023**, *639*, 434–443.
- (24) Li, X.; Liu, Y.; Zhang, Y.; Majonis, D.; Wang, M.; Fashandi, M.; Winnik, M. A. *Chem. Mater.* **2024**, *36* (17), 8174–8187.
- (25) Huang, Z.; Xie, X.; Wu, Y.; Liu, R.; Lv, Y. *J. Am. Chem. Soc.* **2025**, *147* (6), 4904–4914.
- (26) Delgado-Gonzalez, A.; Sanchez-Martin, R. M. *Anal. Chem.* **2021**, *93* (2), 657–664.
- (27) Pulsipher, K. W.; Dmochowski, I. J. *Isr. J. Chem.* **2016**, *56* (9–10), 660–670.
- (28) Liu, X.; Theil, E. C. *Acc. Chem. Res.* **2005**, *38* (3), 167–175.
- (29) Edwardson, T. G. W.; Levasseur, M. D.; Tetter, S.; Steinauer, A.; Hori, M.; Hilvert, D. *Chem. Rev.* **2022**, *122* (9), 9145–9197.
- (30) Jutz, G.; van Rijn, P.; Santos Miranda, B.; Böker, A. *Chem. Rev.* **2015**, *115* (4), 1653–1701.
- (31) Song, N.; Zhang, J.; Zhai, J.; Hong, J.; Yuan, C.; Liang, M. *Acc. Chem. Res.* **2021**, *54* (17), 3313–3325.
- (32) Zhang, B.; Tang, G.; He, J.; Yan, X.; Fan, K. *Adv. Drug Delivery Rev.* **2021**, *176*, No. 113892.
- (33) Liu, G.; Wu, H.; Wang, J.; Lin, Y. *Small* **2006**, *2* (10), 1139–1143.
- (34) Liu, G.; Wu, H.; Dohnalkova, A.; Lin, Y. *Anal. Chem.* **2007**, *79* (15), 5614–5619.

- (35) Yin, X.; Chen, B.; He, M.; Hu, B. *Microchimica Acta* **2019**, *186* (7), 424.
- (36) Wu, H.; Engelhard, M. H.; Wang, J.; Fisher, D. R.; Lin, Y. *J. Mater. Chem.* **2008**, *18* (15), 1779–1783.
- (37) Mastour Tehrani, S.; Lin, W.; Rosenfeldt, S.; Guerin, G.; Lu, Y.; Liang, Y.; Drechsler, M.; Förster, S.; Winnik, M. A. *Chem. Mater.* **2016**, *28* (2), 501–510.
- (38) Rheinländer, A.; Schraven, B.; Bommhardt, U. *Immunol. Lett.* **2018**, *196*, 22–32.
- (39) Nicholas, K. J.; Greenplate, A. R.; Flaherty, D. K.; Matlock, B. K.; Juan, J. S.; Smith, R. M.; Irish, J. M.; Kalams, S. A. *Cytometry Part A* **2016**, *89* (3), 271–280.